Archives of Materials Science and Engineering

Volume 82
Issue 2
December 2016
Pages 49-56

International Scientific Journal published monthly by the World Academy of Materials and Manufacturing Engineering

Influence of 65G steel microstructure on crack faces friction factor under mode II fatigue fracture

Y.L. Ivanytskyj [a], T.M. Lenkovskiy [a], Y.V. Molkov [a], V.V. Kulyk [b,*], Z.A. Duriagina [b,c]

[a] Karpenko Physico-Mechanical Institute of the National Academy of Sciences of Ukraine, Naukova St., 5, Lviv 79060, Ukraine

[b] Department of Applied Materials Science and Materials Engineering, Lviv Polytechnic National University, Ustyyanovych str., 5, Lviv, 79013, Ukraine

[c] The Jhon Paul II Catholic University of Lublin, Al. Racławickie 14, 20-950 Lublin, Poland

* Corresponding e-mail address: kulykvolodymyrvolodymyrovych@gmail.com

ABSTRACT

Purpose: The aim of the paper is to evaluate the dependence of microstructure parameters, strength and plasticity of steel on crack faces friction factor.

Design/methodology/approach: The specimens for the investigation were cut out from the 10 mm thick hot-rolled plate of 65G steel used as a model material for fatigue and durability testing of whole-rolled railway wheels. The mechanical characteristics of the steel were determined according to the state standard using cylindrical specimens of diameter 5 mm and effective length 50 mm. The specimens were heat-treated at the mentioned conditions. Fatigue testing under mode II loading was carried out on a special rigid loading machine in the standard laboratory conditions at symmetric sinusoidal cycle with a frequency of 12 Hz in the range of fatigue crack growth rates $da/dN = 5 \cdot 10^{-8} \ldots 5 \cdot 10^{-7}$ m/cycle until its reaches relative length $l/b \geq 0.8$. The obtained microsections were investigated using the optical metallographic microscope Neophot 9 equipped with a digital camera Nikon D50 and electronic scanning microscope Zeiss EVO 40XVP. Hardness of the specimens with different microstructure was determined using durometer TK-2. The crack faces friction factor was determined using original device for fractured surfaces sliding under certain compression force realization.

Findings: The dependences of microstructure parameters, strength and plasticity of steel on crack faces friction factor are obtained.

Research limitations/implications: The investigation of the influence of microstructure parameters, strength and plasticity of real wheel steels on crack faces friction factor at the mode II fatigue crack growth will be carried out.

Practical implications: The value of crack faces friction factor have strong impact on stress intensity at the crack tip and must be taken into account at crack growth rates curves plotting.

Originality/value: Mode II fatigue crack faces friction factor of steel is firstly experimentally determined.

Keywords: Microstructure; 65G steel; Transverse shear; Fatigue fracture; Crack faces friction factor

Reference to this paper should be given in the following way:

Y.L. Ivanytskyj, T.M. Lenkovskiy, Y.V. Molkov, V.V. Kulyk, Z.A. Duriagina, Influence of 65G steel microstructure on crack faces friction factor under mode II fatigue fracture, Archives of Materials Science and Engineering 82/2 (2016) 49-56.

MATERIALS

1. Introduction

The investigation of fatigue fracture of steels for solid rolled railway wheels under transverse shear (mode II fracture) and fatigue crack growth rate curves plotting for crack growth resistance evaluation is a topical problem [1-3]. Unlike normal tension (mode I fracture) at transverse shear the crack faces are in constant contact, that causing the appearance of friction forces during their mutual motion. As the calculation models [4-12] show this has an effect on the stress-strain state at the crack tip and significantly decreases the stress intensity factor (SIF) K_{II} and its range ΔK_{II}. However, it is known [4,7] that the value of friction forces at the faces of a real shear crack depends not only on the applied stresses and the material friction factor, which is classically evaluated for polished surfaces by the standard procedures [13], but also on the relief of fracture surface, formed in the process of fatigue crack propagation. In this case the geometrical parameters of the crack faces surface and mechanical characteristics of steel are determining ones that in its turn depends on steel phase composition and microstructure. In this paper the crack faces friction (CFF) factor was experimentally determined. The proposed technique takes into account the topography of crack faces surface that was formed under cyclic transverse shear. The dependence between steel structural state and CFF value was established too.

2. Experimental procedures

The mode II fatigue crack growth was implemented on an I-beam specimen (Fig. 1) used for the fatigue crack growth resistance of materials evaluation under transverse shear [2,11,14].

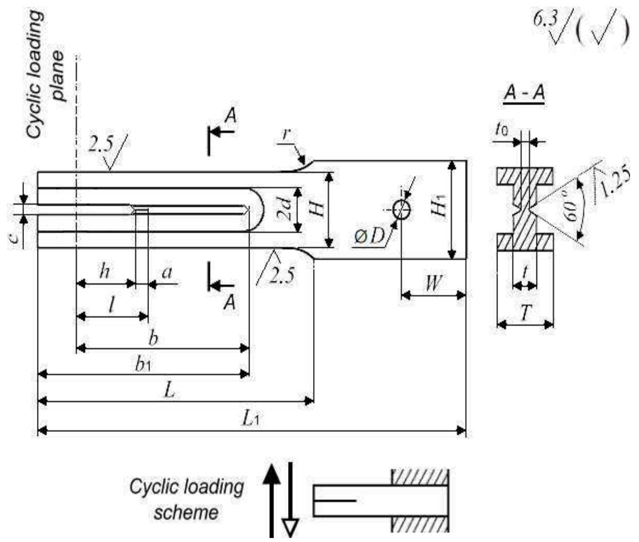

Fig. 1. A specimen for crack growth resistance evaluation of materials under transverse shear

Specimens were cut out from the 10 mm thick hot-rolled plate of 65G steel (analogues 1066, 1566, 66Mn4, Ck67, 080A67, 65Mn, G15660) used as a model material for fatigue fracture and durability testing of whole-rolled railway wheels [2]. The chemical composition of this steel is given in Table 1. To get different microstructures of steel a series of specimens with dimensions $L_1 = 180.0$ mm; $H_1 = 32.0$ mm; $r = 20.0$ mm; $L = 110.2$ mm; $W = 27.0$ mm; $D = 6.0$ mm; $H = 27.8$ mm; $T = 9.6$ mm; $b_1 = 87.8$ mm; $b = 72.0$ mm; $2d = 15.9$ mm; $c = 1.4$ mm; $t = 3.2$ mm were quenched from 820°C in oil and tempered at temperatures 600°C, 500°C, 400°C and 300°C for 1 h, after which a side notch of a length of $h = 25.2$ mm and V-like grooves to $t_0 = 1.1$ mm was made.

Table 1.
Composition of 65G steel

Chemical element	C	Si	Mn	Ni	Cr	Cu	S	P
Wt Pct	0.62…0.7	0.17…0.37	0.9…1.2	< 0.25	≤ 0.25	≤ 0.2	≤ 0.035	≤ 0.035

The mechanical characteristics of the steel were determined according to the state standard [15] using cylindrical specimens of diameter 5 mm and effective length 50 mm. The specimens were heat-treated at the mentioned conditions.

For steel microstructure evaluation the segments of size 5 x 5 mm from the mounting side of specimens were cut out and longitudinal microsections were prepared. Microsections were etched by 4% nitric acid solution in isoamyl alcohol at temperature 20°C according to [16] by rubbing the surface with a wad of cotton wool for 5…10 s and later washing in ethyl alcohol. The obtained microsection was investigated using the optical metallographic microscope Neophot 9 equipped with a digital camera Nikon D50 and electronic scanning microscope Zeiss EVO 40XVP.

Hardness of the specimens with different microstructure was determined using durometer TK-2.

Fatigue testing under mode II loading was carried out on a special rigid loading machine [17] in the standard laboratory conditions at symmetric sinusoidal cycle with a frequency of 12 Hz in the range of fatigue crack growth rates $da/dN = 5\cdot10^{-8}...5\cdot10^{-7}$ m / cycle until its reaches relative length $l / b \geq 0.8$.

To determine the CFF factor f_c the previously proposed approach was used [11]. The fragments of length 70 mm each including fatigue crack faces were cut out from the fractured specimens (Fig. 2a) and tested as a friction pair according to Coulomb-Amonton's law by a special device (Fig. 2 b, c). One fragment of the specimen was fixed by gripers to the supporting plate, and the other with a drilled hole in the wall was placed on the first one in such a manner to ensure their full contact along the fatigue fracture surface.

Then, the upper fragment was loaded with weights of 2 kg, 6 kg, 10 kg and 15 kg and was shifted by force F, applied to the hole. The change of force in time was recorded by personal computer using a tensometric dynamometer and analog-digital transducer E-440 with software PowerGraph 3.3.8. From the obtained dependences "time-force" the critical shift force F at which the upper fragment starts moving on the lower one, was found. Having the pressure force P_N and shear force F the CFF factor f_c was calculated by formula: $f_c = F / P_N$. For each pressure force P_N the value of f_c was calculated by the results of three tests.

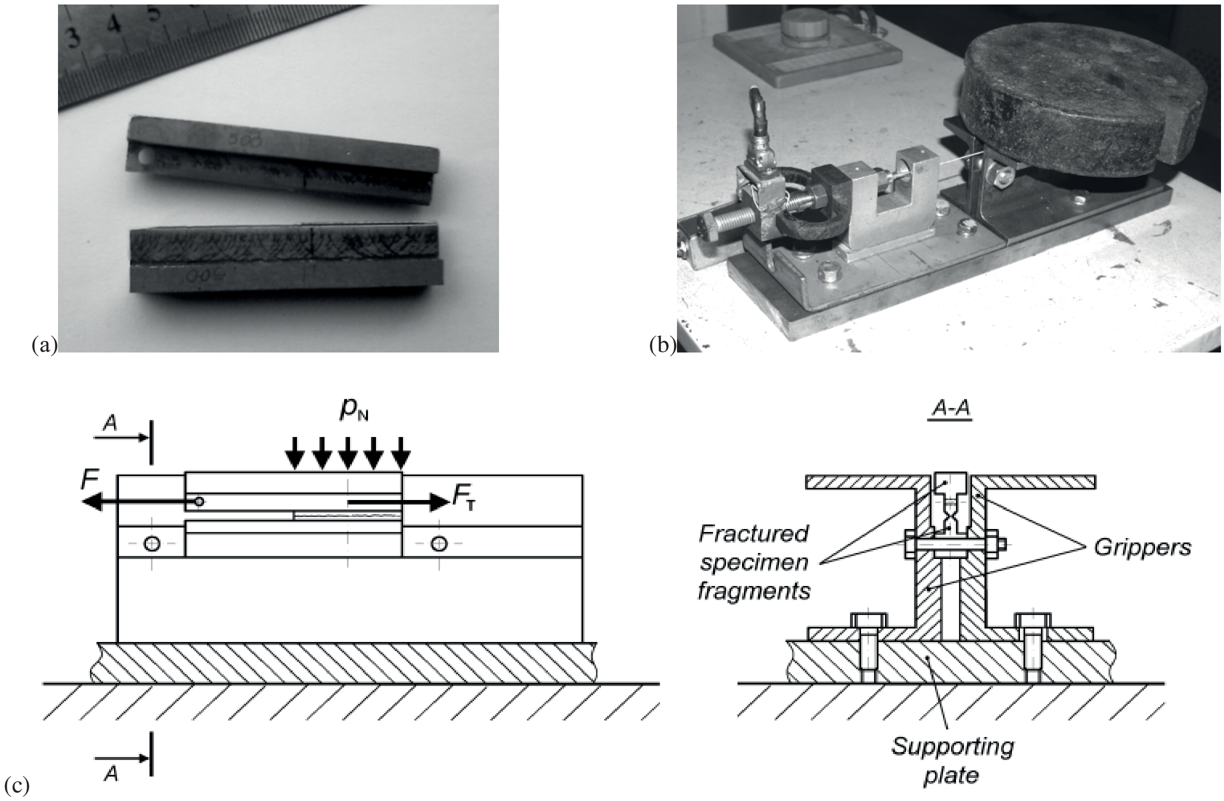

Fig. 2. Fragments of the fractured I-beam specimen (a), device for determing the CFF factor (b), and its working scheme (c)

3. Results and discussion

At the quenching and tempering at different temperatures takes place the diffusion process of martensite decomposition and carbide transformation. As a result of that the ferrite-cementite microstructures of different dispersion and morphology are formed (Fig. 3). Thus, under tempering at 600°C a tempered martensite microstructure (Fig. 3 a) has the form of lamellar, sometimes nodular cementite formations of irregular shape that forming groups of size 10…20 µm in the ferrite matrix. The result of tempering at 500°C is tempered martensite microstructure (Fig. 3 b) with lamellar irregular shape cementite formations of size 6…12 µm appearing in the ferrite matrix. When the tempering temperature decreases from 400°C to 300°C the cementite groups of size 4…8 µm and 2…5 µm, respectively, are formed (Fig. 3 c, d). These groups have an exclusively irregular lamellar shape.

As it is seen from the obtained results (Table 2) the decrease of the tempering temperature from 600°C to 300°C leads to a more fine microstructure (in about 4 times), thus increasing the hardness in 1.7 times and decreasing plasticity in almost 2 times.

The evaluated CFF factor f_c of steel with different microstructures varies in a wide range (Table 3). Based on the obtained results the dependence of CFF factor f_c on the strength characteristics of steel (Fig. 4), plasticity characteristics (Fig. 5) and also on the average size of cementite groups in a microstructure (Fig. 6 a) and hardness of steel (Fig. 6 b) are plotted.

As we can see the decrease of cementite groups size increases the CFF factor. Since the steel microstructure dispersion determines its mechanical characteristics, it is evident that the improvement of the steel mechanical characteristics and hardness causes the increase of CFF factor.

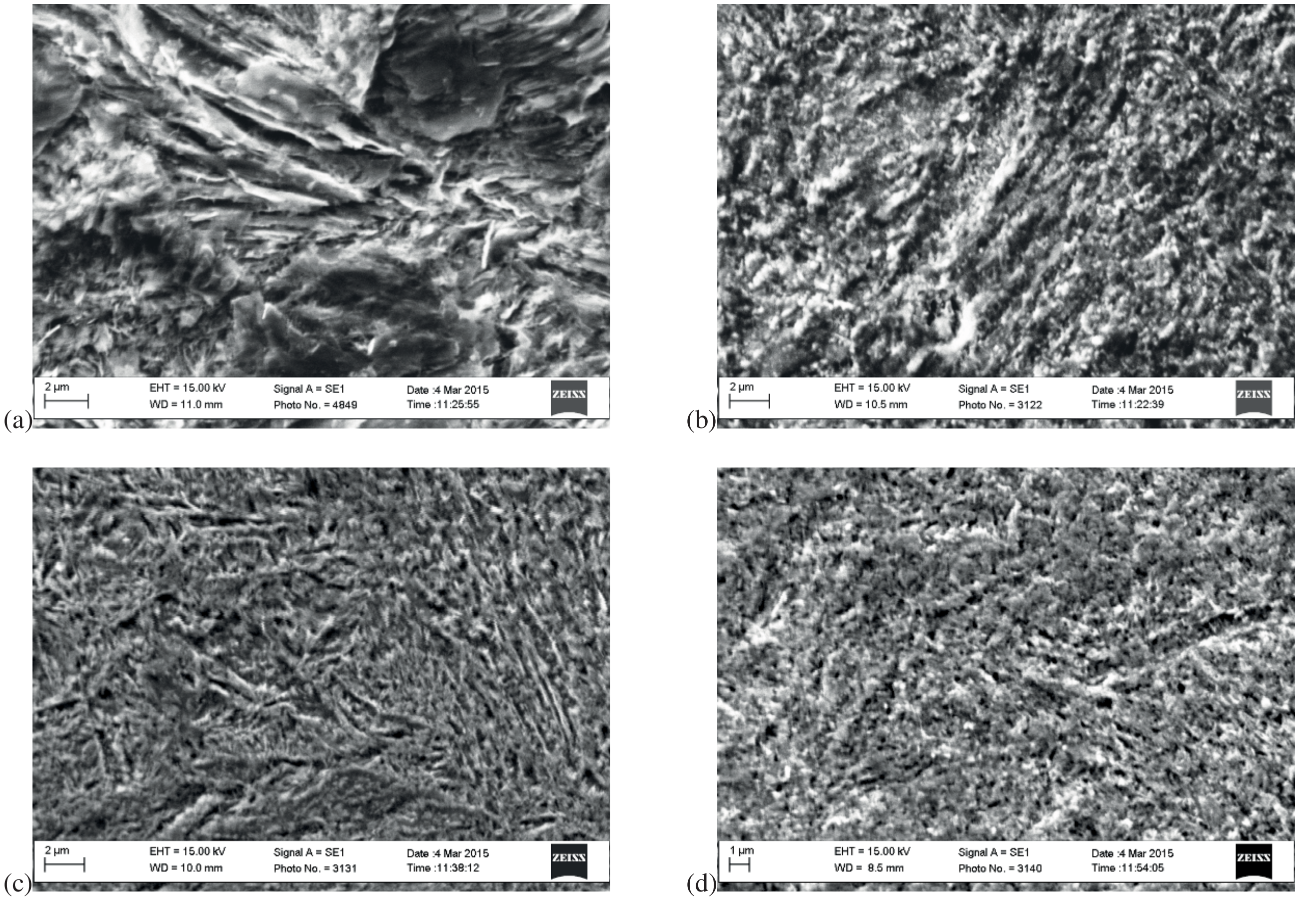

Fig. 3. Microstructure of 65G steel after quenching from 820°C in oil and tempering for 1 h at temperatures: 600°C (a), 500°C (b), 400°C (c), and 300°C (d)

Table 2.
Mechanical properties of 65G steel in different structural states

Quenching with tempering at temperature t_{temp}, °C	Size of cementite groups d_c, μm	Mechanical properties				
		Yield stress σ_{ys}, MPa	Ultimate stress σ_{ult}, MPa	Elongation δ_{10}, %	Reduction of area ψ, %	Hardness *HRC*
600	10…20	910	1050	14	48	32
500	6…12	1160	1320	10	34	39
400	4…8	1530	1680	8	28	44
300	2…5	1810	2120	6	27	54

Table 3.
Crack faces friction factors of 65G steel in different structural states

Tempering temperature t_{temp}, °C	600	500	400	300
CFF factor f_c	0.48	0.72	0.84	0.96

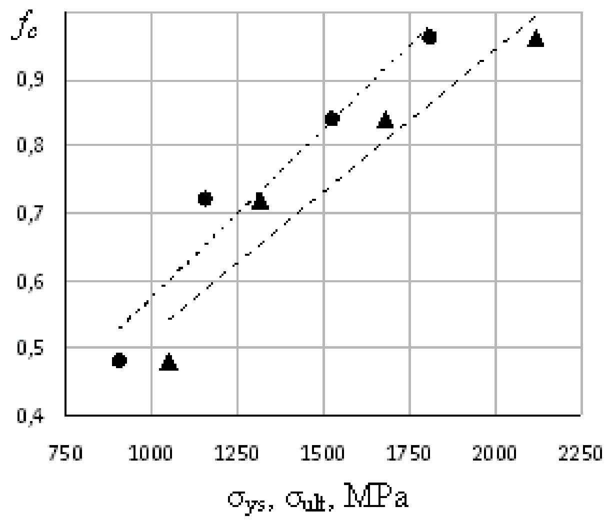

Fig. 4. Influence of yield stress (●) and ultimate stress (▲) of the 65G steel on CFF factor

It should be noted that at the transverse shear crack propagation its faces are exposed to intensive wear. Since the crack faces surfaces near its mouth has a longer history of loading, it is obvious that they are more worn than areas near the crack tip. The surfaces near the mouth are smoother and fitted to each other, and the surfaces near the crack tip have a rough relief.

By visual observations on I-beam specimens fatigue fracture was found that in unloaded position there is a gap between the crack faces. At the fatigue crack growth rate is near $da/dN = 10^{-7}$ m / cycle this gap was approximately 0.15 mm for crack length 11.5 mm (Fig. 7 a). At the same time in the area near the crack tip the faces were closed and the gap was not visible. At the maximal loading of cycle crack faces are in tight contact with each other without a gap throughout the crack length. Under these conditions occurs steadily grinding of crack faces due to their relative displacement. The wear product (debris) in the form of a dispersed powder (Fig. 7 b) always excretes out the gap and sticks to the V-like groove surface.

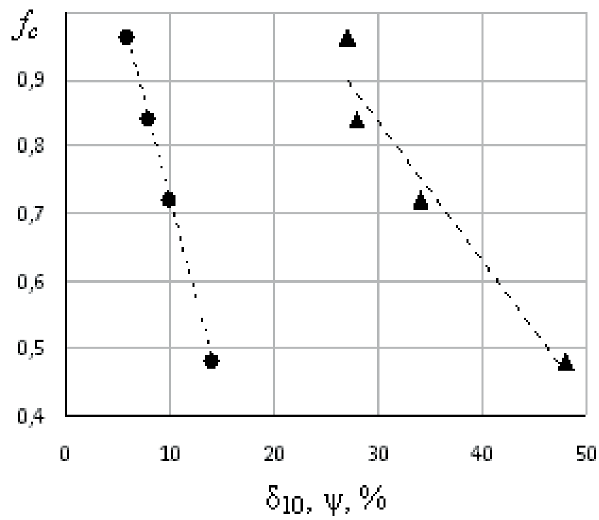

Fig. 5. Influence of elongation (●) and reduction of area (▲) of the 65G steel on CFF factor

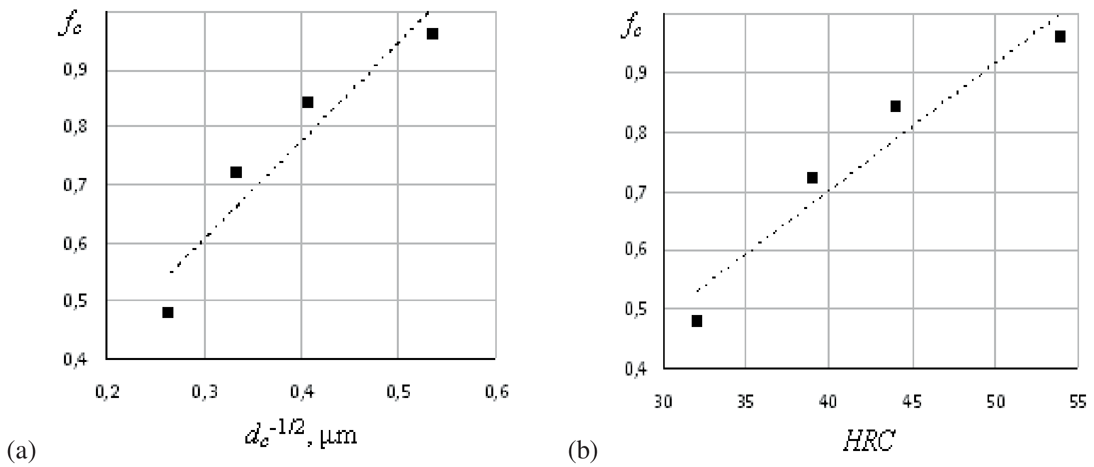

Fig. 6. Influence of cementite groups size in microstructure (a) and hardness (b) of the 65G steel on CFF factor

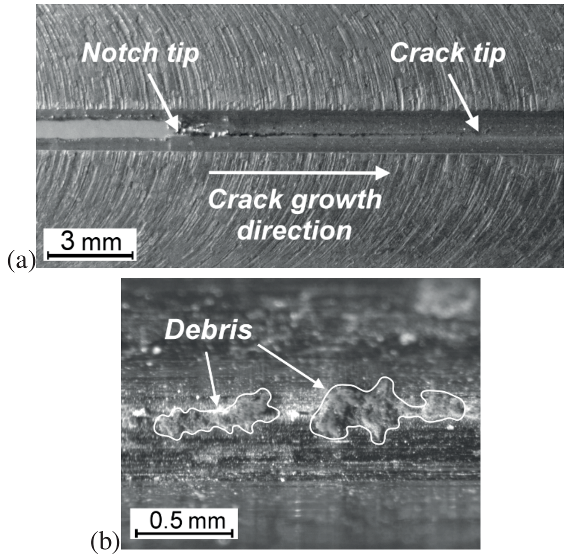

Fig. 7. Mode II fatigue crack in unloaded I-beam specimen (a) made of tempered 65G steel (t_{temp} = 500ºC) and wear debris on the bottom of V-like groove near crack tip (b)

Based on these considerations it is evident that the CFF factor near the tip and near the mouth of crack is different. At the crack tip it is maximal, and at the mouth it is minimal. Taking into account the results of experimental investigation of friction factor change in the process of machine parts getting ground [18], it can be said that in the crack tip CFF factor is 1.2 ... 1.6 times higher than in the mouth. This greatly depends on a number of mechanical, physical and chemical factors that are very difficult to take into account in a terms of macroscale crack theory. So, it is useful to accept the average value of CFF factor in calculation. In the works, which deal with the evaluation of durability and residual lifetime of machine parts with mode II cracks the same value of CFF factor in all areas of crack faces for materials with various structures is used. In [5] was accepted f_c = 1, in [6] f_c = 0.6, in [9] f_c = 0.5, in [10] f_c = 0.3, in [19] f_c = 1 and in [20] f_c = 0.4. For this reason, the averaged value of CFF factor obtained in this study is determining one for the evaluation of stress-strain state of bodies with transverse shear cracks.

Therefore, the evaluation of influence of the crack faces friction on stress intensity factor at transverse shear is very important. Fig. 8 shows the dependence between SIF K_{II} and averaged CFF factor at compression of Brazilian disc specimen obtained in [8]. According to dependences obtained from finite differences solution it can be seen that for f_c = 1 K_{II} is reduced on average by 40%, and for f_c = 0.5 by 20%. It should be noted that an increase of the relative crack length the quantitative impact of f_c on the K_{II} practically unchanged.

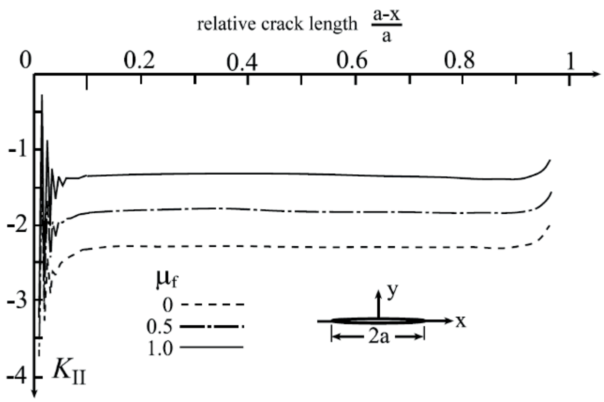

Fig. 8. Normalized stress intensity factor K_{II} calculated by displaced method for crack friction factor μ_f = 0, 0.5 and 1 [8]

Fig. 9 presents similar dependence obtained in [6] for cantilever specimen with chevron net section. For crack lengh 5 mm it is established that f_c = 0.4 reduces K_{II} by 40%, f_c = 0.6 almost by 60% and f_c = 1 by 70%. For shorter cracks this impact is even more substantial. Similar dependences (Fig. 10) were built for I-beam specimen (Fig. 1), which was used in this study and the similar trends were obtained. So it can be said that in all cases f_c decreases K_{II}.

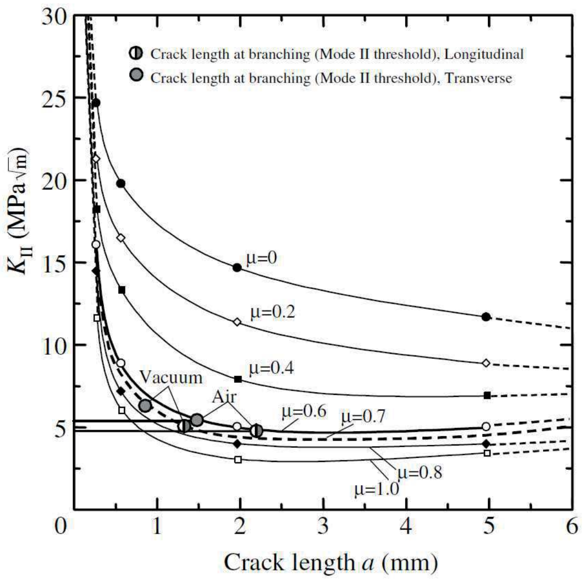

Fig. 9. Relastionship between mode II crack length and stress intensity factor for various crack faces friction factor μ obtained by FEM [6]

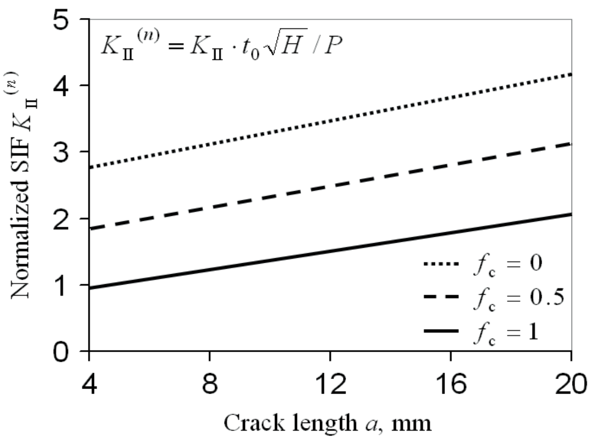

Fig. 10. CFF factor f_c influence on normalized stress intensity factor $K_{II}^{(n)}$ for various crack length a in I-beam specimen

4. Conclusions

On the base of the investigations performed it was found that with the increase of microstructure dispersion and strength of the 65G steel the transverse shear crack faces friction factor increases and with the increase of plasticity characteristics – it decreases. Increase of the hardness also increases the transverse shear crack faces friction. It is established, that the crack faces friction factors under transverse shear obtained in this study is in 3…5 times higher than the value obtained for polished surfaces by standard technique. Presented results can be used in stress intensity factor calculation for transverse shear cracks in steel with different microstructure. It will allow a correct plotting of fatigue crack growth rate curves and will increase the accuracy of the fatigue crack growth resistance characteristics determination.

References

[1] V.V. Panasyuk, O.P. Ostash, O.P. Datsyshyn, et al, Service durability of railway high-strength steel wheels. In: Problems of life time and safety of operation of structures, constructions and machines. Kyiv: Paton Electric welding institute of NASU, 2009, 659-663 (in Ukrainian).

[2] V.V. Panasyuk, O.P. Ostash, I.M. Andreiko et al, Standards for steel for prevention of operation defects on rolling surfaces of solid-rolled high-strength railway wheels. In: Problems of life time and safety of operation of structures, constructions and machines. Kyiv: Paton Electric welding institute of NASU, 2012, 659-663 (in Ukrainian).

[3] O.P. Ostash, V.H. Anofriev, I.M. Andreiko, L.A Muradyan., Kulyk V.V. On the concept of selection of steels for high-strength railroad wheels. Mater. Sci. 48(6) (2013) 697–709.

[4] M. Olzak, J. Stupnicki, Variability of the stress intensity factor during the rolling load on the treadmill with crack, Proceedingsof the 7th National Conference on Fracture Mechanics, Kielce-Cedzyna, Poland, 1999 110-116 (in Polish).

[5] Y. Murakami, C. Sakae, S. Hamada, Mechanism of rolling contact fatigue and measurement of ΔK_{IIth} for steels, In: J.H. Beynon, M.W. Brown, T.C. Lindley et al (ed) Engineering Against Fatigu, Rotterdam: A. A. Balkema, 1999, 473-485.

[6] Y. Murakami, Y. Fukushima, K. Toyama, S. Matsuoka, Fatigue crack path and threshold in Mode

II and Mode III loadings. Engineering Fracture Mechanics. 75/3-4 (2008) 306-318.
[7] O. Darchuk, Modelling of fatigue crack surface interaction under mode II loading, Proceedings of the 3th International Conference on Fracture Mechanics of Materials and Structural Integrity, Lviv, Ukraine, 2004 311-316 (in Ukrainian).
[8] A. Dorogoy, L. Banks-Sills, Effect of crack face contact and friction on Brazilian disk specimens-A finite difference solution, Engineering Fracture Mechanics 72 (2005) 2758-2773.
[9] P. Navratil, P. Skalka, P. Damborsky, M. Kotoul, Crack propagation in railway rim in a case of rectilinear ride, Proceedings of the 4th International Conference on Crack Paths, Gaeta, Italy, 2012, 1007-1014.
[10] V.V. Panasyuk, O.P. Datsyshyn, Material Damages and Life Time of Solids under a Cyclic Contact. Procedia Materials Science 3 (2014) 1250-1256.
[11] Y.L. Ivanyts'kyi., T.M. Lenkovs'kyi, V.M. Boiko, S.T. Shtayura, Methods for the construction of the kinetic diagrams of fatigue fracture for steels under the conditions of transverse shear with regard for the friction of crack lips, Journal of Materials Science 49(6) (2014) 749-754.
[12] O.P. Datsyshyn, A.Y. Hlazov, A.B. Levus, Specific Features of Contact of the Faces of an Edge Crack Under Moving Hertzian Loads, Journal of Materials Science 49/5 (2014) 589-601.
[13] State Standard GOST 27640-88, Engineering materials and lubricants, Experimental evaluation of coefficient of friction, Moscow: Standards Publishing, 1998, 21 (in Russian).
[14] P.S. Kun, S.T. Shtayura, T.M. Lenkovs'kyi, Determination of the Stress Intensity Factor for a Transverse Shear Crack in a Beam Specimen, Journal of Materials Science 50/2 (2014) 212-216.
[15] State Standard GOST 1497-84 Metals, Methods of tension test. Moscow: Standards Publishing, 1984, 36 (in Russian).
[16] M. Beckert, H. Klemm, Handbook of metallographic etching methods. Moscow: Metallurgy, 1988, 400 (in Russian).
[17] Y.L. Ivanyts'kyi., S.T. Shtayur., T.M. Lenkovs'kyi. et al., Installation for the Formation of a Mode II Fatigue Crack in Beam Specimens, The patent of Ukraine no. 73715, 19 (2012) 4 (in Ukrainian).
[18] T.A. Stolarski, Tribology in Machine Design. Butterworth-Heinemann, 1990, 298.
[19] K. Aslantas, S. Tasgetiren, Edge Spalling Formation in a Plate due to Moving Compressive Load, Turkish Journal of Engineering and Environmental, 27/5 (2003) 333-338.
[20] M. Guagliano, L. Vergani, Prediction of the Propagation of an Internal Crack under Rolling Contact Loads by a Weight Function Approach., Key Engineering Materials 251/252 (2003) 473-484.